Electronic Supplementary Material (ESI) for Organic & Biomolecular Chemistry

Supporting Information

Highly Selective and Sensitive *in-vivo* Fluorosensor for Zinc(II) without cytotoxicity.

Tarun Mistri, Malay Dolai, Debrup Chakraborty, Anisur Rahman Khuda-Bukhsh, Kalyan Kumar Das and Mahammad Ali*

Address: Department of Chemistry, Jadavpur University, Kolkata 700 032, India; Department of Botany, Kalyani University, Kalyani, 700 032, India

Contents

1. Experimental Section:

A. Instruments

All fluorescence studies were carried out in Perkin Elmer (Model LS-55) spectrophotometer and UV-vis absorption spectra were recorded in Diode array spectrophotometer (Model : Agilent

2453). NMR and mass spectra were recorded in Bruker instrument (500 MHz). The ESI-MS was recorded on Qtof Micro YA263 mass spectrometer.

X-ray Crystallography: The crystal structure of the compound **1**, has been determined. X-ray diffraction data were collected at 273K on a Bruker SMART APEX-II CCD X-ray diffractometer using graphaite-monochromated MoK_{α} radiation (λ =0.71073 Å). The intensity data were corrected with the *SAINT* software package[1]. The structure was solved by direct and Fourier methods and refined by full-matrix least-squares based on F^2 using the *SHELXL* software package.[2]

B. Materials: All solvents used for synthesis purpose were of reagent grade (Merck) unless otherwise noted. For spectroscopic (Uv-Vis. & fluorescence) studies HPLC grade THF and double distilled water were used. Metal salts such as perchlorate of Na^+, K^+, Ca^{2+}, Mg^{2+}, Fe^{2+}, Co^{2+}, Ni^{2+}, Cu^{2+}, Zn^{2+}, Pb^{2+}, Cd^{2+}, Hg^{2+} were purchased from Sigma-Aldrich and used as received All other compounds were purchased from commercial sources and were used as received.
2,6-diformylphenol was prepared according to the literature procedures[3].

C. Scheme and detail of Syntheses:

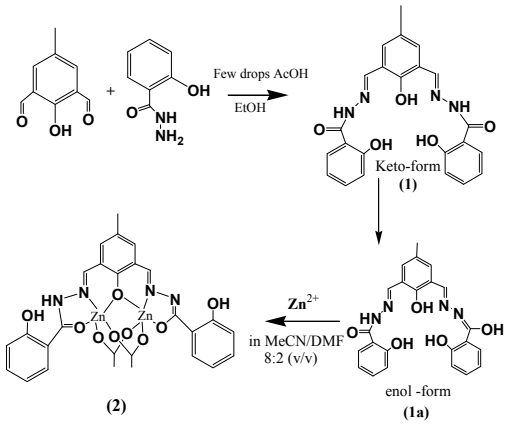

Scheme-I

Detailed procedure for the synthesis of Ligand.

2,6-Diformyl-4-methylphenol was synthesized according to published procedure starting from *p*-cresol.[3] To a solution of 2,6-Diformyl-4-methylphenol(0.328gm,2mmol) in 30 mL of ethanol was added salicylhydrazide (0.608gm,4mmol) in 20 mL of same solvent in presence of 2 drops of acetic acid under boiling condition. After 2 h of stirring pale-yellow precipitates obtained were filtered off, washed several times with cold ethanol/ether (1:1)to obtain pure product in

solid and dried over P_2O_5 under vacuum (yield 85%). CHN analysis for $C_{23}H_{20}N_4O_5$ (M.W. 432) exptl. (calcd.): 64.04(63.88%); 4.85(4.63%); 12.76(12.96%). ES^+-MS(M/Z): 455 ($L+Na^+$) **[Fig. S3]**. ^{1}H-NMR: ^{1}H-NMR 2.31(s, 15-H), 6.96-7.90 (m, aromatic protons); 8.73 (s, 5-H); 12.06-12.26 (-OH protons). Please consult **Fig. S1** for ^{1}HNMR

Detailed procedure for the synthesis of Zn-complex.

A 10 mL of acetonitrile/DMF (8:2 V/V)solution of zinc(II) acetate dehydrate (0.145gm, 0.66 mmol) was added dropwise to a magnetically stirred 20 mL acetonitrile/DMF(8:2 V/V) solution of ligand(1) (0.129gm,.3mmol) for 20 mints at room temperature. The reaction mixture was refluxed for 1h, whereby a greenish-yellow solution was formed. It was filtered and kept in air at room temparature. Pale yellow single crystals of Zn-complex suitable for X-ray crystallography diffraction were obtained on slow evaporation of the filtrate at room temperature after 2 weeks.(64% yield). CHN analysis for $C_{33}H_{38}N_6O_{11}Zn_2$ (M.W. 825.47) exptl. (calcd.): 48.01(47.97%); 4.85(4.60%); 10.76(10.17%). ES^+-MS (M/Z): 887.65 (2 + MeCN+ Na^+)[**Fig. S4**]. ^{1}H-NMR: 2.22(s, 3H(a)], 1.98 [s, (b) 6H], 2.71 and 2.88 [s, (c), 12H], 6.81-7.34 [m, (d) + (i), 9H]; 7.92 [m, (g) + (e), 4H]; 8.60 [(f). 2H] ; 13.5 [b, (h), 2H] [**Fig. S2]**.

2. ^{1}H NMR spectrum of **Ligand (1) and Zn-complex (2).**

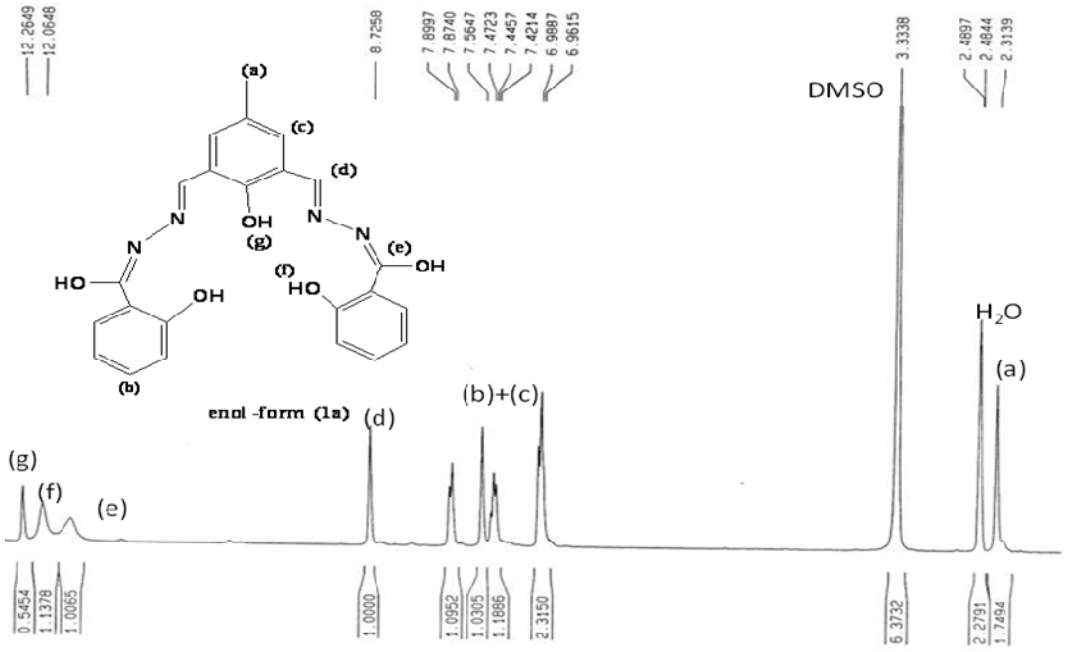

Fig. S1. ^{1}H NMR spectrum of **Ligand (1) in DMSO-d_6, Intrument Bruker 500 MHz**

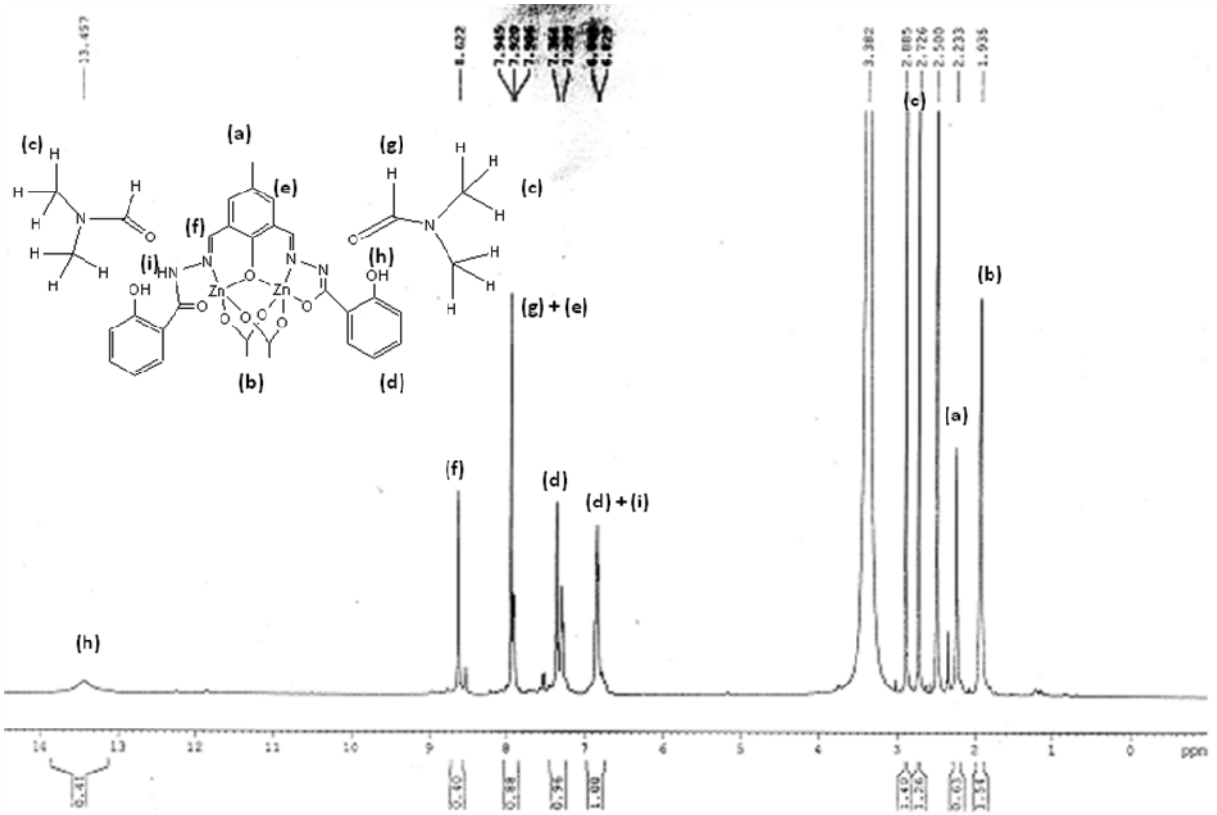

Fig. S2. 1H NMR spectrum of **Zn-complex in in DMSO-d_6, Intrument Bruker 500 MHz**

3. Mass spectrum of **Ligand (1) and Zn-complex (2)**

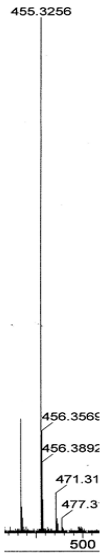

Fig. S3. ESI-MS$^+$ (M/Z) of **1**

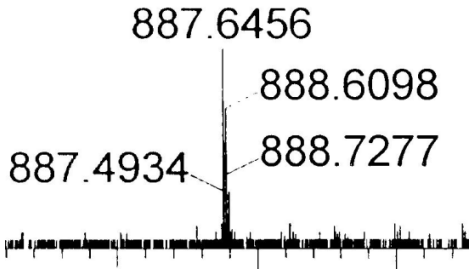

Fig. S4. ESI-MS$^+$ (M/Z) of **Zn-complex:**

4. Absorption titration of Zn^{2+} with 1.

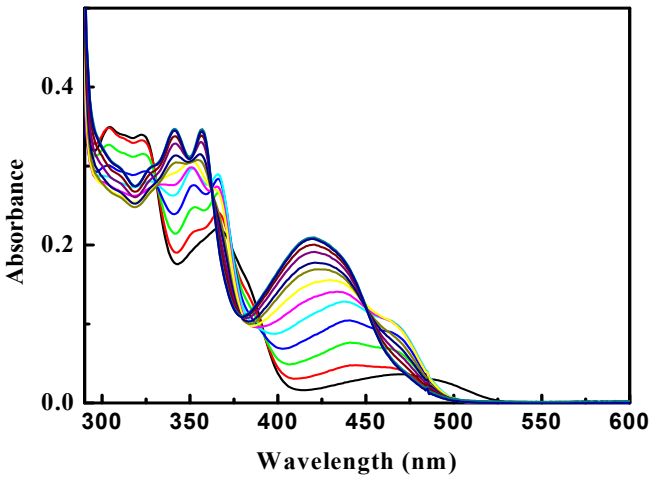

Fig. S5. Change in absorption spectra of **1** (10 μM) upon addition of Zn^{2+} in HEPES buffer of pH 7.0 in H_2O:THF = 4:6 v/v at 25° C, [Zn^{2+}] = 2- 30 μM.

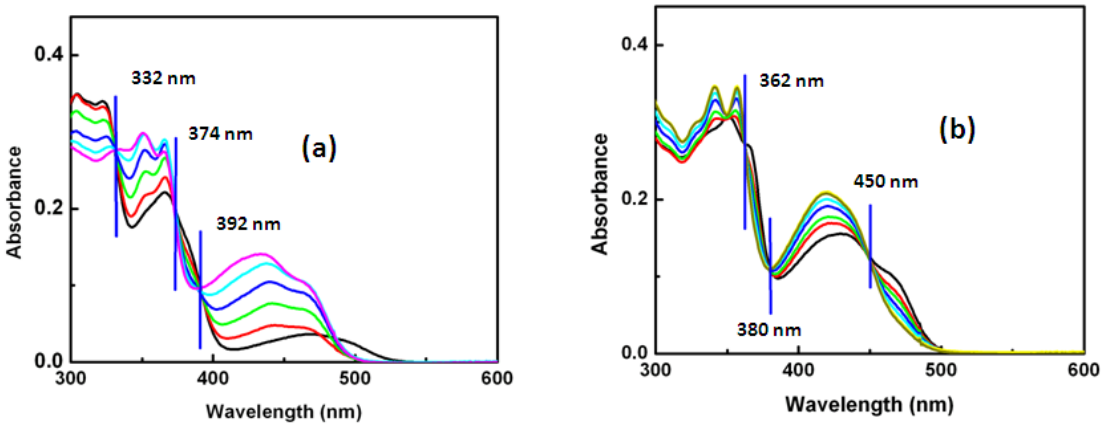

Fig. S5a. Absorption titration of **1** with Zn^{2+}. Conditions: [**1**] = 10.0 μM, (a) [$2n^{2+}$] = 0, 2, 4, 6, 8 and 10 μM; (b) 12, 14, 16, 18, 20, 22,24,26,28, and 30 μM in THF/H_2O v/v(6:4) at p^H= 7(HEPES buffer]

5. Fluorescence titration of 1 with Zn^{2+}

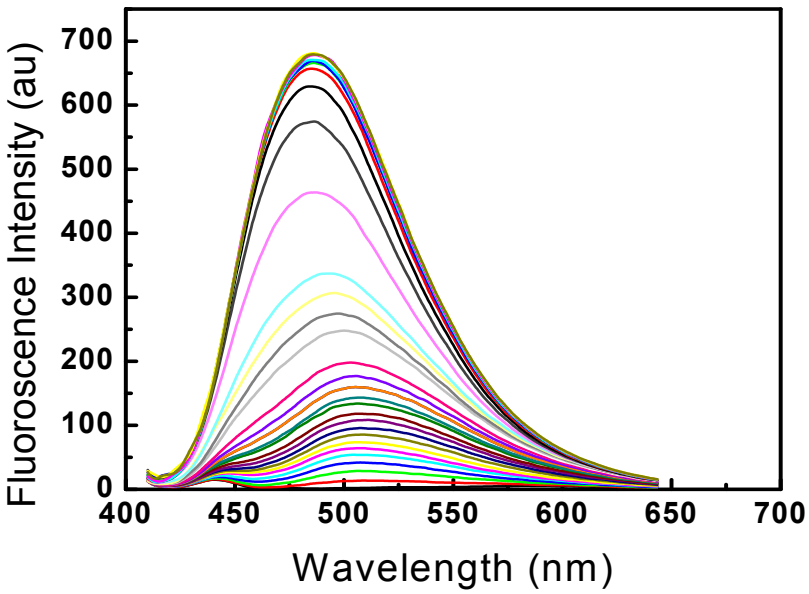

Fig. S6. Change in fluorescence spectra (λ_{ex}) 390 nm of **1** (1.0 μM) upon addition of Zn^{2+} in HEPES buffer of pH 7.0 in H_2O:THF = 4:6 v/v at 25° C), $[Zn^{2+}]$ = 2- 30 μM

6. **Benesi-Hildebrand plot with applied equation.**

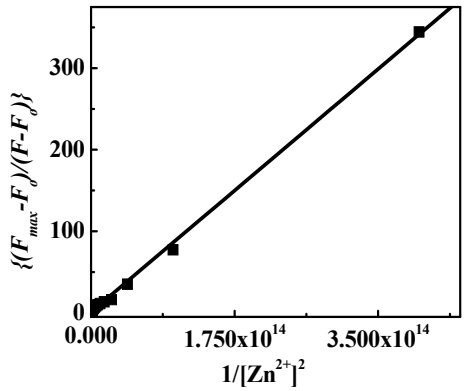

2

Fig. S7. Benesi-Hildebrand plot of $\{(F_{max}-F_o)/(F-F_o)\}$ vs. $1/[Zn^{2+}]^2$.

Benesi-Hildebrand equation is given as:

$$\frac{(F_{max} - F_0)}{(F-F_0)} = 1 + \frac{1}{K\,[Zn^{2+}]^2}$$

F_0 is the fluorescence of **1** in the absence of externally added Zn^{II}, F is the fluorescence obtained at different $[Zn^{2+}]$ (λ_{ex} = 390 nm and λ_{em} = 490 nm] and with F_{max} is the fluorescence of **1** at $[Zn^{2+}]$ in large excess. K (M^{-2}) is the association constant. As shown in **Figure S7**, the plot of $\{(F_{max}-F_0)/(F-F_0)$ *vs.* $1/[\ Zn^{2+}]^2$ shows a liner relationship with slope = (8.51± 0.06) x 10^{-13}, indicating that **1** indeed associates with Zn^{2+} in a 1:2 stoichiometry and intercept = (1.07 ± 0.48) manifesting the self-consistency of the experimental data.

7. Cell imaging experiment:

Cell line and cell culture:

A375 human melanoma cell line was collected from National Centre for Cell Science, Pune, India. A375 cells were cultured in DMEM supplemented with 10% FBS (Invitrogen Corp., USA) and 1% antibiotic (Invitrogen Corp., USA) at 37°C in a humidified incubator (Thermo Electron Corporation) with 5% CO_2. Cells were rinsed with phosphate-buffered saline (PBS; Invitrogen, USA), and incubated with HEPES buffer (p^H 7) containing 10 μM zinc sensor for 30 min at 37 °C and photographs were taken under fluorescence microscope. Then a solution of 10 μM of zinc perchlorate was added onto the cells, and kept at room temperature for 10 min after which photographs were taken. This step of adding zinc perchlorate on the cell suspension was repeated twice after 10 min, and at each step photographs were taken. Then we added the zinc inhibitor

(100 μM) onto the cells and after every 5 min photographs were taken. The same colony of cells had been chosen for all the fluorescence imaging study.

The intracellular Zn^{2+} imaging behavior of zinc sensor was initially studied on A375 human melanoma cancer cells by fluorescence microscopy. After incubation with zinc sensor [10 μM in HEPES] at 37^0C for 10 min, the cells displayed intra-cellular fluorescence (**Fig. S8**.), indicating the sensing ability of the sensor inside cell. The cells exhibited more intense fluorescence when the zinc chlorate was introduced onto the cells (Figure …c,d,e), with increasing fluorescence responses of zinc sensor with further addition of various concentrations of the zinc chlorate solution, which could be evident from the cellular imaging. However, the fluorescence of the cells was deeply suppressed.

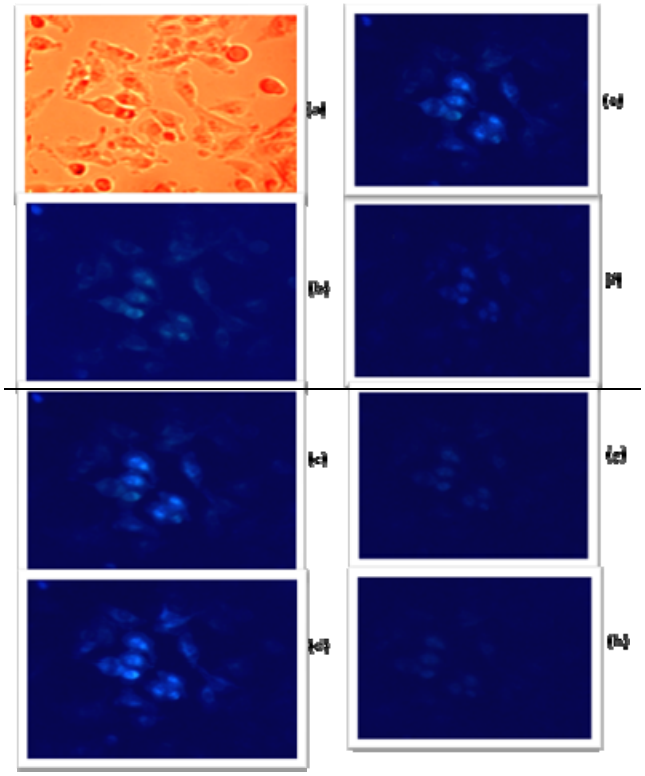

Fig. S8. Fluorescence microscopic observations: (a) Phase contrast and (b) fluorescence images of A375 cells induced by intracellular Zn^{2+} when incubated with 10 μM zinc sensor for 30 min at 37^0 C in HEPES buffer at pH 7.0 and washed with PBS. Cells were exposed sequentially to the increased concentrations of extracellular Zn^{2+} as (c) 10 μM, (d) 20 μM and (e) 30 μM. Return of intracellular Zn^{2+} to the resting level (f-h) achieved by the addition of zinc sensor inhibitor (TEPN, 100 μM), at 5 min interval. For all imaging, the samples were excited at ~360 nm.

8. Cytotoxicity study:

Cell cytotoxicity assay:

To test the cytotoxicity of zinc sensor, 1, 3-(4,5-dimethylthiazol-2-yl)-2,S-diphenyltetrazolium bromide (MTT) assay was performed by the procedure described earlier.[4]

After treatment of the zinc sensor (10, 20, 40, 60, 80 and 100 µM) for 2 h, 10 µL of a MTT solution (1 mg/mL in PBS) was added into each well of a 96-well culture plate and incubated continuously at 37^0 C for 3 h at dark. All media were removed from wells and replaced with 100 µL of acidic isopropyl alcohol. The intracellular formazan crystals (blue-violet) formed were solubilized with 0.04 N acidic isopropyl alcohol, and absorbance of the solution was measured at 595 nm wavelength with a microplate reader. The cell viability was expressed as the optical density ratio of the treatment to control. Values were mean (standard deviation) of three independent experiments. The cell cytotoxicity was calculated as % cell cytotoxicity = 100% - % cell viability. Results are incorporated in **Figure S9**.

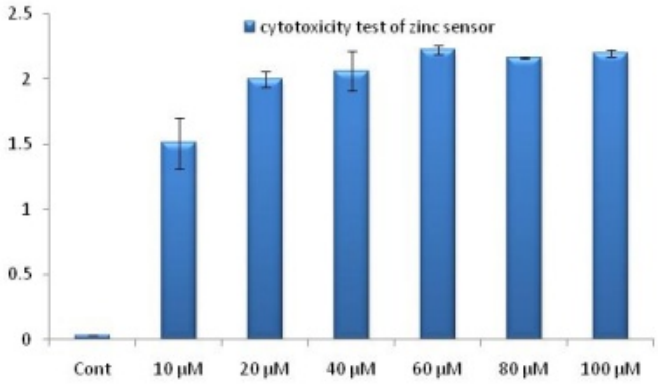

Fig, S9. cytotoxicity assay of zinc sensor: Histogram represents the cytotoxicity of zinc sensor on A375 cells at various concentrations, after 2 h of incubation.

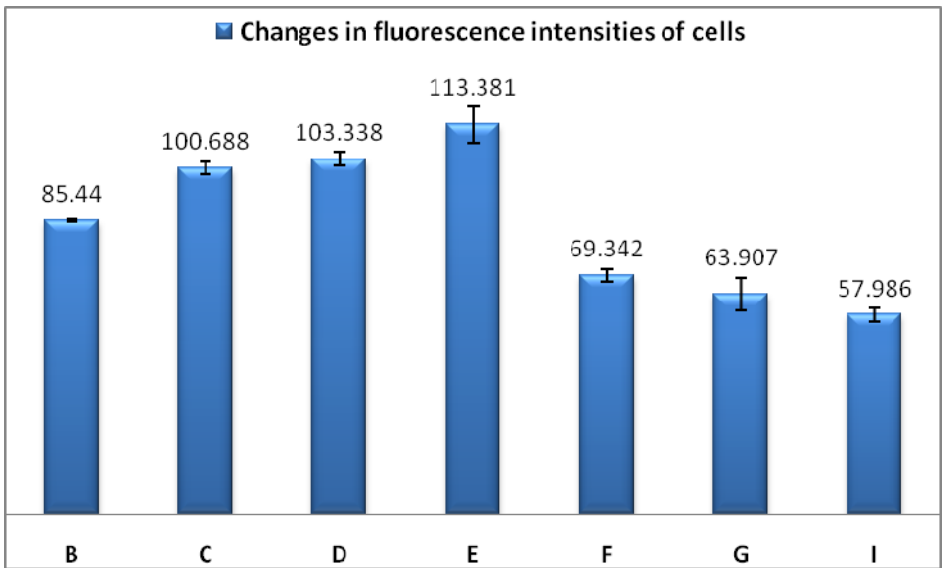

Fig. S10 – Changes in fluorescence intensities of cells in different experimental groups were measured by using 'image J' software. In lane A (not shown in figure) there was no sensor and therefore no fluorescence (0) observed

9. DFT calculation on 2:

DFT calculations on complex **2** were perfomed using Gaussian 03 program.[5] Starting from the X-ray coordinates we have fully optimized the geometries of the $[Zn^{II}(L)(OAc)_2].2DMF$. The B3LYP[6] functional has been adopted along with 6-31+G(d,p) basis set for H, C, N, O atoms and LANL2DZ effective core potentials and basis set for the Zn atom. The global minima of all these species were confirmed by the positive vibrational frequencies. Frontier molecular orbitals of complex **2 is shown in Figure S10.** Bond distances and bond angles around the Zn^{II} centers are in well agreement with the crystallographic data (See Table S1). Time dependent density functional theory (TDDFT)[7,8] with B3LYP density functional was applied to study the low-lying excited states of the complex both in gas phase as well as in THF using the optimized geometry of the ground (S_0) state. The vertical excitation energies of the lowest 20 singlet states are also computed here. The UV spectra computed from TDDFT calculations in THF show three important peaks in the range 270-450 nm (See **Figure S11**). The band around 450 nm is dominated by the HOMO→LUMO excitation, while the band around 370 nm is mainly due to

HOMO→LUMO+1 and HOMO-1 →LUMO transitions. The details of the vertical excitation energies, oscillator strengths, and nature of excitations are shown in **Table S2**.

Table S1. Selected Bond distances and Bond Angles of **2** with DFT calculated values in the parenthesis.

Table S1. Selected Bond distances and Bond Angles of 2

Bond type	**Bond Distance (Å)**	**Bond type**	**Bond angle(°)**
Zn1-O1	1.975 (17) [2.032]		
Zn1-O4	2.050 (15) [2.057]		
Zn1-O6	1.980 (18)[2.031]		
Zn1-O7	2.117(14)[2.271]		
Zn1-N5	2.026(18)[2.115]		
Zn2-O2	1.964 (17)[2.001]		
Zn2-O3	2.141 (16)[2.141]		
Zn2-O5	1.955(17)[2.002]		
Zn2-O7	2.052 (15)[2.152]		
Zn2-N9	2.031(18) [2.144]		
Zn1…Zn2	**3.182 [3.301]**		
Angle types	**Bond angle(°)**		
O7 -Zn1 -N5	86.76(6)[83.58]	O4 -Zn1-O7	164.19(7) 160.82]
O2 -Zn2 -O3	87.03(7) [91.44]	O4 -Zn1-N5	77.90(7) [77.25]
O2 -Zn2 -O5	112.00(7)[123.12]	O6 -Zn-O7	95.81(6) [91.89]
O2 -Zn2 -O7	99.22(6) [99.01]	O6 -Zn1-N5	116.73(8) [123.03]
O2 -Zn2 -N9	122.84(8) [117.7]	O3 -Zn2-O5	90.14(7) [91.32]
O7 -Zn2 -N9	88.37(7)[83.93]	O3-Zn2 -O7	164.27(6) [157.79]
O1-Zn1-O4	91.37(7) [91.83]	O3 -Zn2 -N9	76.17(7) [73.86]
O1 -Zn1-O6	112.23(8) [113.95]	O5-Zn2-O7	100.71(7) [99.12]
O1-Zn1-O7	95.75(6) [98.41]	O5 -Zn2-N9	122.05(8) [117.54

O1 -Zn1-N5	130.43(8) [122.92]	Zn1-O7-Zn2	99.48(6) [96.51]
O4 -Zn1-O6	94.52(7) [98.62]		

Table S2. Vertical excitation energies (E_{cal}), oscillator strengths (f_{cal}), and type of excitations of the lowest few excited singlets obtained from TDDFT calculations of complex 2 in THF (ε=7.58)

compd	state	E_{cal}/nm	f_{cal}	excitation
complex 2	S_1	444	0.3683	HOMO→LUMO (0.67),
	S_2	376	0.6450	HOMO→LUMO+1 (0.57), HOMO–1→LUMO (0.27), HOMO–2→LUMO (0.19), HOMO→LUMO (0.13)
	S_3	365	0.1426	HOMO–1→LUMO (0.61), HOMO→LUMO+1 (0.28)
	S_4	346	0.3263	HOMO–2→LUMO (0.61), HOMO–1→LUMO+1 (0.19), HOMO→LUMO+1 (0.17)
	S_5	331	0.1067	HOMO–1→LUMO+1 (0.59), HOMO→LUMO+2 (0.22), HOMO–2→LUMO (0.22), HOMO–2→LUMO+1 (0.13)
	S_7	313	0.1602	HOMO–2→LUMO+1 (0.47), HOMO→LUMO+2 (0.39), HOMO–3→LUMO (0.27)
	S_{11}	286	0.1173	HOMO–4→LUMO (0.67), HOMO–6→LUMO (0.12)
	S_{13}	278	0.2584	HOMO–6→LUMO (0.64), HOMO–4→LUMO (0.15), HOMO–1→LUMO+2 (0.12), HOMO–4→LUMO+1 (0.10)

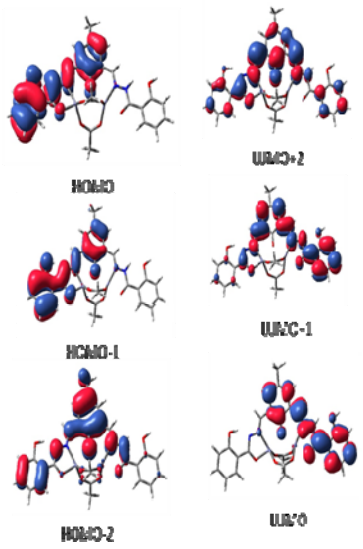

Fig. S10. Frontier molecular orbitals of complex **2**

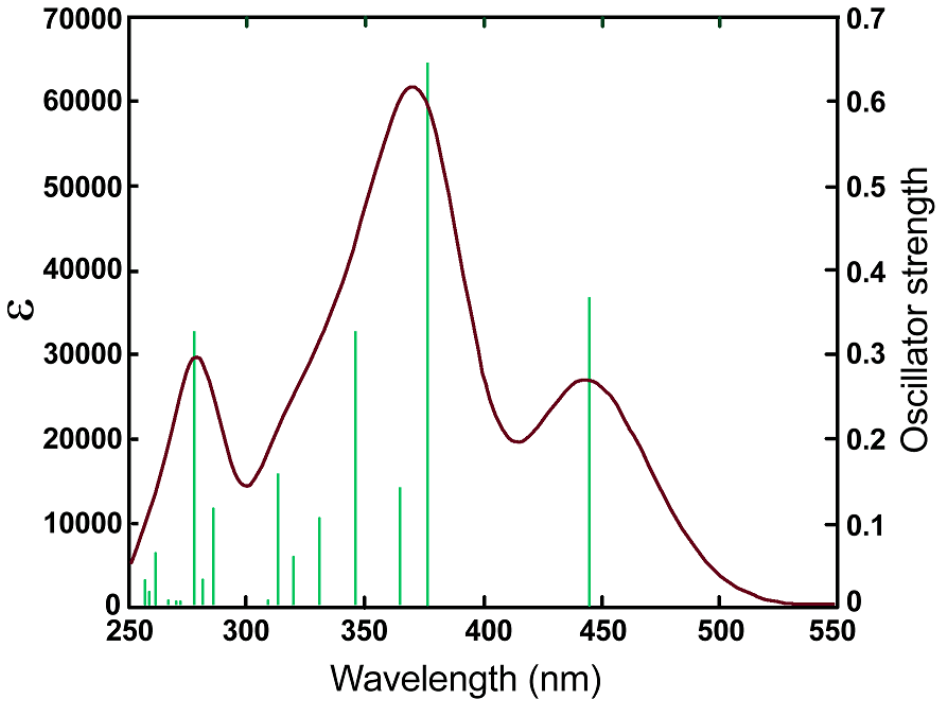

Fig. S11. The UV spectrum computed from TDDFT calculations in THF

10. References

(1) *SAINT,* SMART and SADABS; Bruker AXS Inc; Madison,W I, **2001**.
(2) G. M. Sheldrick, Acta Crystallogr.2008, **A64**, 112.
(3) R. R. Gagne, C. L.Spiro, T. J. Smith, C. A. Hamann, W. R. Thies, A. K. Schiemke, *J. Am. Chem. Soc.* 1981, **103**, 4073.
(4) J. Ratha, K. A. Majumdar, S. K. Mandal, R. Bera, C. Sarkar, B. Saha, C. Mandal, K. D; Saha, R. Bhadra, *Mol. Cell. Biochem*. 2006, **290**, 113.
(5) M. J. Frisch, et al., *Gaussian 03*, revision C.02; *Gaussian*, Inc.: Wallingford, CT, 2004.
(6) A. D.. Becke, *J. Chem. Phys.,* **1**993, **98**, 5648.
(7) P. J.; Hay. W. R. Wadt, *J. Chem. Phys.,* **1**985, **82**,299.
(8) S. Miertus, E. Scrocco, J. Tomasi, *Chem. Phys.* 1981, **55**, 117;; V. Barone, M. Cossi, J. Tomasi, *J. Comput. Chem.*1998, **19**, 404